

# Direct visualization of iron sheath shielding effect in MgB<sub>2</sub> superconducting wires

Alexey V. Pan, Sihai Zhou, Shi Xue Dou, and Hua Kun Liu  
*Institute for Superconducting and Electronic Materials, University of Wollongong,  
Northfields Avenue, Wollongong NSW 2522, Australia*  
(May 3, 2002)

By employing a local magneto-optical technique, we have directly visualized the full screening of superconducting MgB<sub>2</sub> filaments in mono-core and multifilamentary wires by their ferromagnetic iron sheaths in applied magnetic fields up to  $B_a \simeq 0.2$  T. This is in agreement with global magnetization measurements on the same samples. An extended pseudo-Meissner effect is obtained within the range  $|B_a| \leq B_s$ , where  $B_s$  is the saturation field of the magnetization measured in the ferromagnetic iron as a function of  $B_a$ . The screening of the iron sheath can dominate, depending on the magnetic prehistory, in fields up to 1.5 T. At higher fields the superconducting response becomes slightly suppressed by the magnetized sheath.

New promising horizons for superconducting tapes and wires were opened by the discovery of MgB<sub>2</sub> superconductor [1]. MgB<sub>2</sub> wires have been reported to have quite high values of critical current density  $J_c$ , in particular wires sheathed by hard magnetic materials such as iron (Fe) [2–4]. A special procedure for preparation of MgB<sub>2</sub> multifilamentary wires investigated in this work has been shown to be beneficial for increasing  $J_c$  of the wires [4]. Furthermore, ferromagnetic iron has been reported to cause a magnetic shielding effect which, in spite of an initial fear of suppressing the superconductivity, seems to provide an extended range of a constant critical current  $I_c$  at least in an externally applied magnetic field range  $0.2 \leq B_a \leq 0.6$  T at  $T = 32$  K [5]. However, the results did not yet provide satisfactory detailed information on *how* this magnetic shielding affects the superconducting behavior in the wires. In fact, the shielding effect of iron does not allow the external field to reach the superconducting filaments, rather it collects the field inside the iron sheath. This means that the superconductor does not need to screen itself from the field, effectively extending the range of the Meissner state. Moreover, this shielding is expected to eliminate the self-field suppression of  $I_c$  upon the passage of super-current through wires in the absence of the external field. In this letter, by employing a magneto-optical (MO) technique we directly visualize the effect of the iron magnetic shielding in MgB<sub>2</sub> mono-core (MC) and multifilamentary (MF) wires. We show a clear difference between their normal and superconducting states. We also show that the screening is magnetic history dependent and can quite considerably influence the magnetic behavior of the wires in fields up to 1.5 T, so that it cannot be neglected. Above  $B_a \simeq 1.5$  T, iron exhibits a negative influence, slightly suppressing the superconductivity.

The Fe-sheathed MgB<sub>2</sub> superconducting wires were

made by employing the powder-in-tube method and an “in-situ” Mg+2B powder reaction for forming MgB<sub>2</sub> superconductor. A detailed description of the wire manufacturing procedure and its characterization is given elsewhere [4]. The MC and MF wire cross sections are shown in Fig. 1. Transport measurements of the wires provided the critical currents  $I_c = 78.1$  A and 110 A at temperature  $T = 4.2$  K and in zero applied field for the MC and MF wires, respectively. To obtain a magnetic field distribution over the wires with the help of the MO technique, the samples were polished to the final cross sections which are denoted by the black lines in Fig. 1. In the case of the MF wire, only the two filaments denoted by arrows were exposed for taking MO images. An epitaxial ferrite-garnet magneto-optical indicator film with in-plane magnetization was used for the imaging.

Two sets of MO images shown in Figs. 2 and 3 were taken at room temperature (RT) and  $T = 19$  K, the latter one is well below the critical temperature  $T_c = 38.6$  K of the samples, in different fields. As can be readily seen there is no difference between the MO images taken in either the normal or the superconducting state at  $B_a \lesssim 0.1$  T. The images taken below 0.1 T demonstrate that the magnetic field starts to concentrate at the edges of the wire (bright area along the wire edges in Figs. 3a and b). The different widths of the bright area at the edges are due to different angles of the iron edges formed after polishing (see the black line in Fig. 1b). As  $B_a$  is increased, the induced field inside the samples concentrates only in the iron sheath. The applied field is sucked inside the iron sheath from a distance of  $\sim 0.5$  mm outside the wire (see Figs. 3c and d). However, the behavior depends on the amount and mechanical treatment of the iron used for the sheath, which is quite different for our samples. Further away from the wire, the brightness of the gray color corresponds to the field value applied, undisturbed by the magnetic influence of the sample. Generally, the darker the area on the MO images, the lower the magnetic field induced in that region; the brighter the area the higher the field. As can be seen, the two bright areas at the wire edges (Figs. 3a and b) have induced magnetic field higher than the applied field.

At  $B_a > 0.1$  T, a discrepancy between images taken at RT and  $T = 19$  K (Figs. 2c, d and 3c, d) becomes visible. Bright stripes due to induced field, present in the middle of the exposed filaments in both MC and MF wires at RT, disappear in the images taken in the superconducting state ( $T = 19$  K). The presence of the high induction field stripe in the middle of the exposed fila-

ments at RT can probably be explained by the geometry of the iron sheath in vicinity of the filament openings. In the normal state, MgB<sub>2</sub> material is transparent to the magnetic field, therefore it does not influence the distribution of the field inside the wires. Thus, the geometry of the iron in the filament “cavities” acts like a magnifying glass concentrating the magnetic field lines in the middle of the “cavities”. On the contrary, in the superconducting state at  $T = 19$  K, the filaments are strongly diamagnetic, in particular, below the lower critical field  $B_{c1} = (B_c \ln \kappa) / (\kappa \sqrt{2})$ , where  $\kappa$  is the Ginzburg-Landau parameter,  $B_c$  - the thermodynamic critical field. In MgB<sub>2</sub>  $B_{c1} \sim 0.06$  T [6]. By direct comparison with the brightness produced by the applied field far from the wire edges, one sees that the area within the filaments is totally black, which implies that the induced field  $B_i$  in the area is effectively zero (Fig. 2d). In spite the fact that the wires are placed in  $B_a > B_{c1}$ , the filaments are entirely diamagnetic ( $B_i < B_{c1}$  at  $T < T_c$ ), fully expelling the magnetic flux. This extended Meissner state is enabled by iron screening. However, the field expulsion in Fig. 3d is not complete. This is likely to be due to shallow filaments having uneven depth. The black line in Fig. 1b shows that the filament on the left is deeper than the one on the right. This deeper filament clearly shows more complete magnetic flux expulsion. The shallower filament (on the right) when placed in a perpendicular field is expected to be more magnetically transparent simply due to some damage caused by polishing. It is worth mentioning, that upon warming the wires through  $T_c$  in  $B_a = 0.2$  T, we observed the transformation of the image shown in Fig. 3d (below  $T_c$ ) into the one exhibited in Fig. 3c (above  $T_c$ ).

Thus, these local magnetic observations directly show not only the screening effect of the iron sheath above and below  $T_c$ , but also the extended Meissner state of the superconducting filaments, at least in the field range available in our MO setup ( $0 \leq B_a \lesssim 0.2$  T).

Furthermore, after carrying out the local MO experiments we performed global magnetization measurements as a function of the applied field within  $|B_a| < 5$  T at different temperatures with the help of a Quantum Design MPMS SQUID magnetometer. The results of the measurements are presented in Fig. 4 for both MC and MF wires. To enable a comparison between the local and global experiments, the field was applied perpendicular to the polished planes of the wires which is exactly the same orientation used in the MO experiments described above.

At first glance there is no difference in magnetization measurements carried out below (10 and 20 K) and above (45 K)  $T_c$  (Fig. 4c). However, after subtraction of the dominant iron sheath signal measured at  $T = 45$  K, one gets the magnetization behavior at  $T = 10$  and 20 K shown in Fig. 4d, which is attributed to the superconducting response of the filaments. A striking feature of these two curves is the strongly suppressed magnetization within  $|B_a| \lesssim 1$  T. Moreover, within  $|B_a| \lesssim 0.7$  T,

the magnetization is nearly zero. This field interval we refer to as the operation range of the extended pseudo-Meissner state in the MF wire. The region of the suppressed magnetization is well correlated with the ferromagnetic response of iron, showing the saturation of magnetization near  $B_s = |B_a| \simeq 1$  T (Fig. 4c). The saturation occurs when all spins within the magnetic domains of iron become aligned along the applied magnetic field. Below  $B_s$  all the magnetic field energy is spent on the spin alignment, so that no energy is left for affecting the superconductivity inside the filaments. Therefore, the filaments are effectively screened from the applied magnetic field. Above  $B_s$  the magnetic energy starts to influence the superconductivity because it is no longer needed for spin alignment. As a consequence, the extended pseudo-Meissner effect due to the iron screening ceases to exist.

For the MC wire the extended pseudo-Meissner effect disappears already at 0.2 T (Fig. 4b). However, the screening dominates up to 0.5 T, which also correlates with the  $B_s$  value (Fig. 4a) as in the case of the MF wire. A smaller volume of the iron sheath in the MC wire and weaker stress caused by its fabrication might be responsible for the smaller  $B_s$  compared to the MF wire. This again indicates that as long as the magnetic energy of the external field is spent on iron domain remagnetization (up to  $B_s$ ) the magnetic screening of the superconducting filaments dominates.

In the case of the MC wire, unlike the MF wire, we were able to carefully remove the iron sheath. We carried out magnetization measurements of the Fe-sheathed wire and after removal of the sheath. The superconducting volume of the core remained unchanged after the removal. In Fig. 4b we compare these two magnetization curves measured at  $T = 20$  K. In the case of the Fe-sheathed wire (solid circles), we have subtracted the ferromagnetic iron background measured at  $T = 45$  K (Fig. 4a). As can be seen, the magnetization of the Fe-sheathed wire can be larger by a factor of 2 than that for the bare wire above the complete screening region in *increasing*  $|B_a|$ . The magnetization remains higher than that in the bare wire up to  $B_a = 1.5$  T. We believe that this might be an analog of the overcritical state discussed in Ref. [7]. Below 1.5 T, the superconducting response appears to be slightly suppressed by the fully magnetized iron. In *decreasing* field, the superconducting response remains slightly smaller until  $B_s \simeq 0.5$  T. Strictly speaking, we deal here, in contrast to the MO experiments, with a *field cooled* state. This means that the superconducting core might have some frozen magnetic flux inside, ruling out the existence of the pure extended Meissner state as in the case of the MO experiments. That is why we call this state the pseudo-Meissner state.

The origin of the small irreversibility within  $|B_a| \lesssim 0.5$  T in Fig. 4d (compared to the region within  $|B_a| \lesssim 0.2$  T in Fig. 4b) is unclear. The small signal cannot be responsible because of the clear temperature dependence.

The screening effect is also expected to depend on wire geometry. The effects of geometry of a magnetic shell for

a superconducting strip were investigated theoretically in work [7]. However, iron sheath screening in wires offers a much simpler method for commercial production of long cables with an extended range of  $J_c$  unsuppressed by an external magnetic field than the magnetic environment suitable for the strip [7].

In conclusion, we have directly visualized the magnetic screening of the superconducting  $\text{MgB}_2$  filaments in MC and MF wires by means of an iron sheath. The observations showed that the magnetic field induced inside the iron sheath is higher than the applied field. Whereas the superconducting filaments, exhibiting an extended Meissner state, are free from the induced magnetic field at least up to  $B_a = 0.2$  T for both kinds of wires, as revealed by the magneto-optical technique used. Global magnetization measurements showed that the screening effect can be dominant up to  $B_a = 1.5$  T and that it is much more effective upon *increasing*  $|B_a|$  than in decreasing fields.

We would like to thank J. Horvat and T. Silver for careful reading of the manuscript and valuable critical remarks, and M. Tomsic for some assistance. We also benefited from fulfilling discussions with Yu. A. Genenko. This work is financially supported by Australian Research Council.

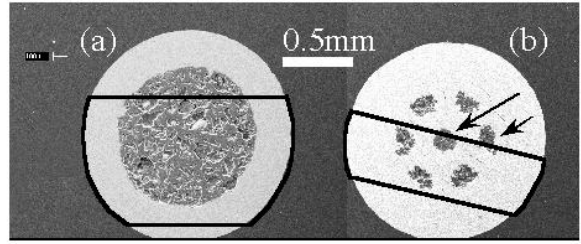


FIG. 1. Cross section of the mono-core (a) and multifilamentary (b) wires. The black lines indicate the remaining parts after polishing.

- 
- [1] J. Nagamatsu, N. Nakagawa, T. Muranaka, Y. Zenitani, and J. Akimitsu, *Nature* **410**, 63 (2001).
  - [2] S. Soltanian, X. L. Wang, I Kusevic, E. Babic, A.H. Li, M.J. Qin, J. Horvat, E.W. Collings, K. Lee, M. Sumption, H. K. Liu, and S.X. Dou, *Physica C* **361**, 84 (2001).
  - [3] M. D. Sumption, E. Lee, E.W. Collings, X. L. Wang, and S. X. Dou, *Proc. of the ICMC 2001 Conference*, Madison, WI, 16-21 July, 2001 (in press).
  - [4] S. Zhou, A. V. Pan, H. K. Liu, and S. X. Dou, (2002) submitted.
  - [5] J. Horvat, X. L. Wang, S. Soltanian, and S. X. Dou, *Appl. Phys. Lett.* **80**, 829 (2002).
  - [6] D. K. Finnemore, J. E. Ostenson, S. L. Bud'ko, G. Lapertot, and P. C. Canfield, *Phys. Rev. Lett.* **86**, 2420 (2001).
  - [7] Yu. A. Genenko, A. Snezhko, and H. C. Freyhardt, *Phys. Rev. B* **62**, 3453 (2000).

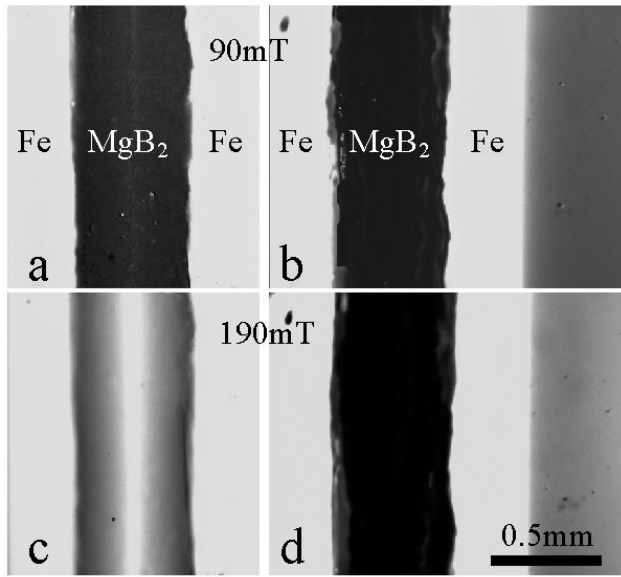


FIG. 2. Magneto-optical images of the Fe-sheathed MC wire at RT (a) and (c), and at  $T = 19$  K (b) and (d) in the magnetic fields as denoted on each row.

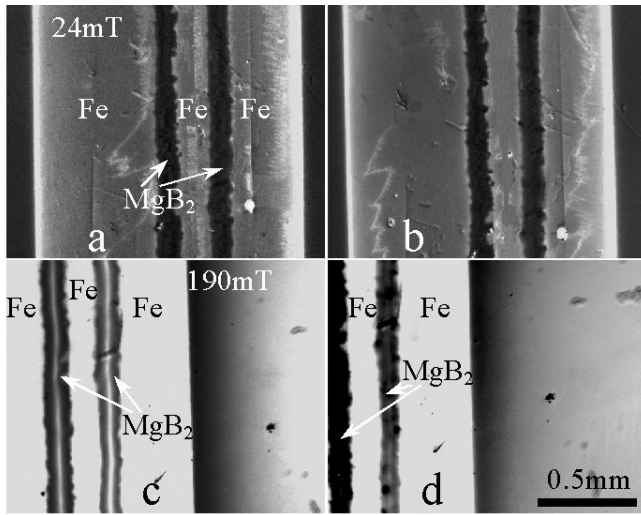


FIG. 3. MO images of the MF wire under the same conditions as described for Fig. 2. Bright zigzag lines in (a) and (b) show a non-relevant domain structure of the MO film.

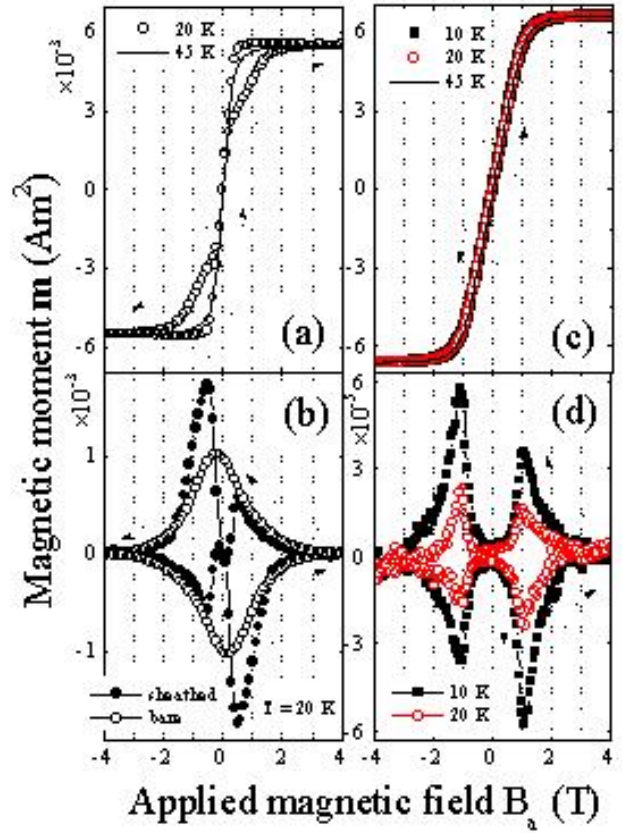


FIG. 4. Magnetization curves of the MC wire measured at  $T = 20$  and  $45$  K (a) and of the MF wire measured at  $T = 10$ ,  $20$ ,  $45$  K (c). (b) Magnetization behavior of the Fe-sheathed MC wire at  $T = 20$  K after subtracting the iron sheath ferromagnetic contribution (solid symbols) and the magnetization measured after having the sheath removed (open symbols). (d) Magnetization of the MF wire at  $T = 10$  and  $20$  K after subtracting the contribution of the iron sheath. Note the  $m$ -scale differences.